Adaptation to Exercise Training in Conduit Arteries and Cutaneous Microvessels in Humans: An Optical Coherence Tomography Study

RADEN ARGARINI[1,2], HOWARD H. CARTER[2], KURT J. SMITH[2,3], LOUISE H. NAYLOR[2], ROBERT A. MCLAUGHLIN[4,5,6], and DANIEL J. GREEN[2]

[1]Physiology Department, Faculty of Medicine, Airlangga University, Surabaya, INDONESIA; [2]Cardiovascular Research Group, School of Human Sciences (Exercise and Sport Science), The University of Western Australia, Perth, AUSTRALIA; [3]Integrative Physiology Laboratory, Department of Kinesiology and Nutrition, College of Health Sciences, The University of Illinois, Chicago, IL; [4]Australian Research Council Centre of Excellence for Nanoscale Biophotonics, Adelaide Medical School, Faculty of Health and Medical Sciences, The University of Adelaide, Adelaide, AUSTRALIA; [5]Institute for Photonics and Advanced Sensing, The University of Adelaide, Adelaide, AUSTRALIA; and [6]School of Electrical, Electronic and Computer Engineering, The University of Western Australia, Perth, AUSTRALIA

ABSTRACT

ARGARINI, R., H. H. CARTER, K. J. SMITH, L. H. NAYLOR, R. A. MCLAUGHLIN, and D. J. GREEN. Adaptation to Exercise Training in Conduit Arteries and Cutaneous Microvessels in Humans: An Optical Coherence Tomography Study. *Med. Sci. Sports Exerc.*, Vol. 53, No. 9, pp. 1945–1957, 2021. **Introduction:** Exercise training has antiatherogenic effects on conduit and resistance artery function and structure in humans and induces angiogenic changes in skeletal muscle. However, training-induced adaptation in cutaneous microvessels is poorly understood, partly because of technological limitations. Optical coherence tomography (OCT) is a novel high-resolution imaging technique capable of visualizing cutaneous microvasculature at a resolution of ~30 μm. We utilized OCT to visualize the effects of training on cutaneous microvessels, alongside assessment of conduit artery flow-mediated dilation (FMD). **Methods:** We assessed brachial FMD and cutaneous microcirculatory responses at rest and in response to local heating and reactive hyperemia: pretraining and posttraining in eight healthy men compared with age-matched untrained controls ($n = 8$). Participants in the training group underwent supervised cycling at 80% maximal heart rate three times a week for 8 wk. **Results:** We found a significant interaction ($P = 0.04$) whereby an increase in FMD was observed after training (post 9.83% ± 3.27% vs pre 6.97% ± 1.77%, $P = 0.01$), with this posttraining value higher compared with the control group (6.9% ± 2.87%, $P = 0.027$). FMD was not altered in the controls ($P = 0.894$). There was a significant interaction for OCT-derived speed ($P = 0.038$) whereby a significant decrease in the local disk heating response was observed after training (post 98.6 ± 3.9 $\mu m \cdot s^{-1}$ vs pre 102 ± 5 $\mu m \cdot s^{-1}$, $P = 0.012$), whereas no changes were observed for OCT-derived speed in the control group ($P = 0.877$). Other OCT responses (diameter, flow rate, and density) to local heating and reactive hyperemia were unaffected by training. **Conclusions:** Our findings suggest that vascular adaptation to exercise training is not uniform across all levels of the arterial tree; although exercise training improves larger artery function, this was not accompanied by unequivocal evidence for cutaneous microvascular adaptation in young healthy subjects. **Key Words:** CUTANEOUS MICROCIRCULATION, EXERCISE TRAINING, OPTICAL IMAGING, CONDUIT ARTERY FUNCTION

Exercise training has beneficial effects on conduit and resistance artery function, structure, and health in humans. Previous studies have shown that training enhances endothelium- and nitric oxide (NO)–mediated function in healthy subjects (1–4) and those with cardiovascular risk factors (e.g., hypertension, hypercholesterolemia, obesity, and diabetes) and diseases (5–7). Functional adaptation can be accompanied, or superseded by, arterial remodeling (2,3,8). Training-induced resistance and conduit artery adaptation occur as a result of localized muscle training (3,9) and also in vascular beds that are not directly involved in the exercise stimulus (4,10,11). The mechanisms responsible for training-induced adaptation are mediated, at least partly, by episodic exposure to increased shear stress (3,4,12) alongside transmural pressure changes during exercise (12,13).

Although robust evidence supports training effects on conduit and larger resistance artery function and remodeling, microvascular adaptation is more difficult to image, quantify, and describe. In skeletal muscle, biopsy studies suggest that

Address for correspondence: Daniel J. Green, Ph.D., School of Human Sciences (Exercise and Sports Science) M408, The University of Western Australia, 35 Stirling Highway, Nedlands, WA 6009, Australia; E-mail: danny.green@uwa.edu.au.
Submitted for publication December 2020.
Accepted for publication February 2021.

0195-9131/21/5309-1945/0
MEDICINE & SCIENCE IN SPORTS & EXERCISE®

DOI: 10.1249/MSS.0000000000002654

exercise training stimulates angiogenesis by promoting growth in the number of capillaries, with consequent increases in capillary density (14), capillary-to-fiber ratio (14,15), and capillary lumen area (15). This adaptation is mediated by angiogenic factors such as vascular endothelial growth factor (14–16), in concert with increases in mechanical forces such as shear stress, and is potentiated by metabolism and hypoxia (16). In contrast to skeletal muscle, less is known regarding training effects on cutaneous microvessels. The cutaneous circulation is an active vessel bed during exercise in humans, responsible for increasing heat dissipation and maintaining body temperature. It has been suggested that skin blood flow may approach 8 $L \cdot min^{-1}$ during whole body heat stress (17), a volume that exceeds resting cardiac output. It might be speculated that intrinsic cutaneous adaptation to repeated exercise exposure could enhance heat dissipation. However, relatively few studies have investigated the effect of exercise training on the skin microcirculation, with mixed results. In cross-sectional studies, people with higher fitness have demonstrated enhanced endothelium-dependent vasodilation in the skin microcirculation compared with less fit controls (18,19). However, other studies did not find such between-group differences (20,21). Wang (22) reported an increase in skin blood flow at rest, in response to incremental exercise and endothelium-dependent vasodilation after 8 wk of exercise training in young healthy, sedentary people. Enhanced NO contribution to skin vasodilation after exercise training was also reported in people with impaired microvascular function, such as sedentary older individuals (23), type 2 diabetes (5), and nonalcoholic fatty liver patients (24), whereas Middlebrooke et al. (25) reported no change in skin microcirculatory function in T2DM after 6 months of aerobic exercise. The endothelial-independent dilation and maximal dilator capacity have been reported to not change (18,23) or decrease (19) with training. Our group recently reported paradoxical *decreases* in peak laser Doppler flowmetry (LDF) responses to a localized heating stimulus after 8 wk of cycle training (26) and also to repeated passive heating (27). We proposed that structural adaptation in the skin microcirculation may account for the decrease in peak red cell flux we observed, with a consequential increase in transit time facilitating heat dissipation. However, this conclusion was speculative because laser Doppler provides indirect and qualitative data relating to averaged cell flux rather than direct visualization of microvessels that would enable quantification of microvessel density, diameter, speed, and angiogenesis (28).

Noninvasive imaging of cutaneous microvessels is a promising approach for early detection of changes in microvascular function and health *in vivo*, because an abundance of skin blood vessels lays superficial beneath the skin surface. It has been proposed that skin microvessel function could reflect generalized microvascular function in humans (28). However, previous skin assessment techniques have not been able to directly visualize and quantify cutaneous microvascular function or structure. We recently developed a noninvasive optical coherence tomography (OCT) technology that provides high-resolution images that enable quantification of the diameter, speed, flow rate, and recruitment of blood vessels in the skin microcirculation to a resolution of ~30 μm. We have published data regarding the feasibility and reproducibility (29,30) of this approach for visualizing and quantifying cutaneous microvascular changes induced by physiological stimuli such as reactive hyperemia (29) and local heating (30). In the current study, we applied this OCT technique to assess the effect of exercise training on cutaneous microvascular adaptation. We hypothesized that exercise training would increase structural indices of skin microcirculation (diameter and density), with consequent decreases in the speed of blood transit through the microcirculation, alongside improvements in conduit artery function, cardiorespiratory fitness, and body composition.

METHODS

Participants

Sixteen young and healthy men were recruited for this study (26.4 ± 4.7 yr, 169.3 ± 5.4 cm, 77.7 ± 14.1 kg, 26.9 ± 3.8 $kg \cdot m^{-2}$) from the local community through advertisement. At study entry, the participants were randomized into control or training groups. Block randomization was used to ensure a balanced number of participants assigned into each group. The inclusion criteria included the following: healthy (free from cardiovascular, metabolic, and respiratory diseases); sedentary or recreationally active (<150 min of exercise per week); nonsmokers; and free from medication or supplements. Baseline participant characteristics and those after 8 wk of intervention are provided in Table 1. This study was approved by The University of Western Australia's Human Research Ethics Committee and conformed to the standards outlined in the Declaration of Helsinki (reference number RA/4/7134). All subjects provided written informed consent before their involvement in this study.

Study Design

Before study commencement, participants visited the laboratory for familiarization with the study protocol and completed a medical history and preactivity questionnaire. Preliminary assessments were undertaken during two different visits: visit 1 for body composition (dual-energy x-ray absorptiometry) and $\dot{V}O_{2max}$ testing, and visit 2 for vascular assessments. All assessments were conducted at the same time of day in a quiet and temperature-controlled (23°C) laboratory in the Cardiovascular and Exercise Research Centre at The University of Western Australia. After preliminary assessment, all participants were asked to maintain their usual level of daily physical activity, whereas participants in the training group underwent additional supervised exercise training, as described hereinafter. All preliminary assessments were repeated after 8 wk of intervention, at least 3 d after the last exercise session to eliminate any acute exercise effects.

Exercise Training Intervention

Participants performed exercise on a stationary bicycle ergometer (Monark Ergomedic 828E, Varberg, Sweden) three

TABLE 1. Participants characteristics.

	Control (n = 8, ♂)		Training (n = 8, ♂)		RM 2-Way ANOVA, P Value		
	Week 0	Week 8	Week 0	Week 8	Time	Group	Interaction
Age, yr	26.4 ± 4.3		26.4 ± 5.3			>0.999 (t-test)	
Blood pressure, mm Hg							
Systolic	118 ± 5	115 ± 6	113 ± 6	108 ± 5*,***	0.01	0.03	0.454
Diastolic	69 ± 6	66 ± 6	65 ± 5	61 ± 4	0.048	0.084	0.791
MAP	85 ± 5	81 ± 5	81 ± 5	77 ± 4*	0.012	0.053	0.813
RHR, bpm	70 ± 10	67 ± 8	66 ± 8	60 ± 3*	0.014	0.118	0.395
Body weight, kg	80.8 ± 15.4	80.9 ± 15.8	74.6 ± 12.9	74.0 ± 13.3	0.646	0.38	0.488
BMI, kg m^{-2}	27.7 ± 4.5	27.7 ± 4.6	26.3 ± 3.2	26.0 ± 3.2	0.545	0.446	0.412
Cardiorespiratory fitness							
$\dot{V}O_{2max}$, mL·kg^{-1}·min^{-1}	29.9 ± 5.7	29.1 ± 5.4	29.7 ± 2.8	36.3 ± 2.6**,****	0.001	0.11	<0.001
HR_{max}, bpm	185 ± 11	179 ± 9*	184 ± 12	178 ± 8*	0.002	0.84	>0.999
$Time_{max}$, min	14.2 ± 1.7	13.5 ± 1.6	13.7 ± 2.3	16.9 ± 3.4**,****	0.038	0.177	0.003
$Power_{max}$, W	147 ± 19.8	143 ± 14.1	165 ± 33.4	185 ± 33.4 **,****	0.037	0.038	0.005

Values are mean ± SD.
*P < 0.05, week 0 vs week 8 within the same group.
**P < 0.01, week 0vs week 8 within the same group.
***P < 0.05, control vs training at the same time point.
****P < 0.01, control vs training at the same time point.
RM, repeated-measures.

times per week across an 8-wk period. Each session of exercise consisted of 30 min of cycling at 80% of maximal heart rate (HR_{max}), derived from a maximal exercise test undertaken before the exercise training (see discussion hereinafter). Our exercise intervention in this study was based on the American College of Sport Medicine guidelines on cardiorespiratory exercise training (31). After a 5-min warm-up, subjects were supervised to maintain their target heart rate in the cadence of 60 rpm by adjusting the workload accordingly. A Polar H10 (Polar, Kempele, Finland) heart rate monitor was used to continuously monitor heart rate during each exercise session. A total of 24 exercise sessions were performed in the supervised laboratory.

Cardiorespiratory Fitness ($\dot{V}O_{2max}$) Assessment Protocol

Participants performed a maximal exercise test (ramp protocol) until volitional fatigue to determine their $\dot{V}O_{2max}$. The test was performed on an electronically braked cycle ergometer (Lode, Groningen, Holland). All tests were performed under similar conditions (23°C, 54% relative humidity). After a 5-min warm-up at 50 W and self-selected cadence, the incremental test commenced. Workload was increased by 20 W every 2 min, and subjects were allowed to choose their preferred cadence within the range of 70–90 rpm. Rate of perceived exertion was assessed at the end of every stage, before each workload was progressed. Verbal encouragement was given to the subjects to continue the test until volitional exhaustion. The test was terminated when the subject was unable to consistently maintain a pedal cadence greater than 70 rpm. During the test, minute ventilation, oxygen uptake ($\dot{V}O_2$), carbon dioxide production, and fraction of oxygen and carbon dioxide were recorded over 15-s epochs using an automated metabolic cart system (TrueOne®2400; ParvoMedics, Salt Lake City, UT). Gas analyzers were calibrated before each test using room air and a certified gas mixture (4% CO_2, 16% O_2, balance N_2; Airgas Healthcare, Miami, FL) and a metered 3-L syringe (Hans Rudolph Inc., Shawnee, KS) in accordance with the manufacturer's instructions. $\dot{V}O_{2max}$ was defined by the following criteria: 1) oxygen consumption failed to increase linearly with an increase in workload, 2) RER was greater than 1.1, and 3) HR achieved >90% age-predicted HR_{max}. $\dot{V}O_{2max}$ was recorded as the highest reading averaged over four consecutive epochs. $\dot{V}O_{2max}$ was reported normalized by body weight (in milliliters per kilogram per minute).

Anthropometry and Body Composition Assessment

Body weight and height were measured using an electronic scale (CPWplus-200; ADAM Instruments, Oxford, CT) and a stadiometer, with participants wearing light clothes and no shoes. Body mass index (BMI) was calculated as body weight (in kilograms) divided by height (in meters squared). Body composition (fat and lean mass) and bone density were analyzed using dual-energy x-ray absorptiometry (Lunar Prodigy; GE Medical Systems, Madison, WI), calibrated daily; fat mass, visceral adipose tissue, lean body mass, and bone mineral density were assessed.

Vascular Assessments

Before the vascular assessment, participants were asked to fast for 6 h and abstain from alcohol, tea, caffeine, and chocolate 12 h before test (32,33). They were also asked to avoid exercise or vigorous activity for 24 h before each test.

Conduit artery endothelial function assessment: flow-mediated dilation. After instrumentation and 20-min of supine rest, blood pressure and heart rate were obtained (Dinamap V100; GE Healthcare, Chicago, IL). After this, conduit artery endothelial function was assessed in the brachial artery using the flow-mediated dilation (FMD) method, in accord with well-established guidelines (32), which are briefly summarized hereinafter.

The right arm was extended and supported using a contoured foam pad. A pneumatic cuff was placed around the forearm, distal to the olecranon process, and connected to a rapid

inflated/deflated pneumatic device (D.E. Hokanson, Bellevue, WA) to induce local ischemia. An ultrasound probe (15 MHz), attached to high-resolution vascular ultrasound machine (t3200 system; Terason, Burlington, MA), was placed on the upper arm. Once an optimal image of the brachial artery was obtained, the probe was held stable and ultrasound parameters were set to optimize longitudinal B-mode images of the lumen–arterial wall interface. Along with the artery diameter, continuous Doppler velocity was collected using the lowest possible insonation angle (<60°). After 1 min of baseline recording (Camtasia Studio 8; Techsmith, Okemos, MI), the pneumatic cuff on the forearm was inflated simultaneously to suprasystolic level (220 mm Hg) for 5 min. Ultrasound recording resumed 30 s before cuff deflation and continued for a further 3 min. All data were saved as video files (.avi) for posttest analysis.

Posttest analysis of artery diameter and velocity was undertaken using customized edge-detection and wall-tracking software. Our coefficient of variability using this software is 6.7%, and the reproducibility of analysis is significantly better than manual methods (34). Brachial artery FMD was presented as the relative dilation from the preceding resting diameter (in percent), whereas arterial flow was calculated as area under the curve (AUC) at baseline and also during the peak response immediately after the cuff pressure (in milliliters per minute). We calculated the shear rate stimulus responsible for endothelium-dependent FMD as area under the shear rate curve (SR_{AUC}) from cuff deflation to the point of maximal arterial dilation.

Skin microvascular assessment: LDF and OCT. The experimental preparation is illustrated in Figure 1. Microvascular assessment was performed using a seven-element array LDF probe (model 413, Periflux System 5000; Perimed), with OCT (Telesto III; Thorlabs GmbH, Bergkirchen, Germany) measures assessed simultaneously. Both techniques collected data at rest and in response to two different physiological stimuli: reactive hyperemia and local skin heating. Reactive hyperemia elicits sensory nerve (35) and NO-independent endothelium-mediated vasodilation (36), whereas local heating stimulates axonal reflex and NO-mediated dilation (37). Beat-to-beat continuous arterial blood pressure and heart rate were recorded throughout each session using a Finometer PRO (NOVA; Finapres Medical Systems, Enschede, The Netherlands) with finger cuffs placed on the contralateral arm. LDF and blood pressure/heart rate data were exported to a data acquisition system (PowerLab, LabChart 8; ADInstruments, Colorado Springs, CO) for offline analysis. Skin conductance was calculated as LD flux/mean arterial pressure (PU·mm Hg^{-1}).

The OCT imaging system has a central wavelength of 1300 nm and an axial resolution of 5 μm in tissues (assuming a refractive index of 1.43 for the skin). The lateral resolution of the OCT scanning probe (LSM03; Thorlabs) is 13 μm. This scanning probe was affixed to customized three-dimensional printed spacer (Form2; Formlabs, Somerville, MA) to ensure a standard distance between probe and skin surface. A thermostatic probe holder (PF450; Perimed, Stockholm, Sweden) was fitted inside the custom spacer, allowing the OCT imaging to be performed through it during localized heating (Fig. 1).

The skin sites for microvascular assessment were shaved 24 h before the assessment. A small drop of ultrasound gel was placed between the skin and a transparent square microscope slide (8 × 8 mm) attached to the thermostatic probe holder. This provided a flat imaging surface, eliminating imaging artifacts due to the surface shape of the subject's skin (38). LDF and OCT probe holders were positioned on the ventral forearm using double-sided adhesive rings, adjacent of each other (distance <5 cm), with a skin temperature sensor (MLT; ADInstruments, Bella Vista, NSW, Australia) placed between the probe holders. After positioning the probe, Henna dye was placed around the outer diameter of each probe holder to tattoo the site for repeat placement after the interventions. Once the test was completed, the participant's forearm was wrapped

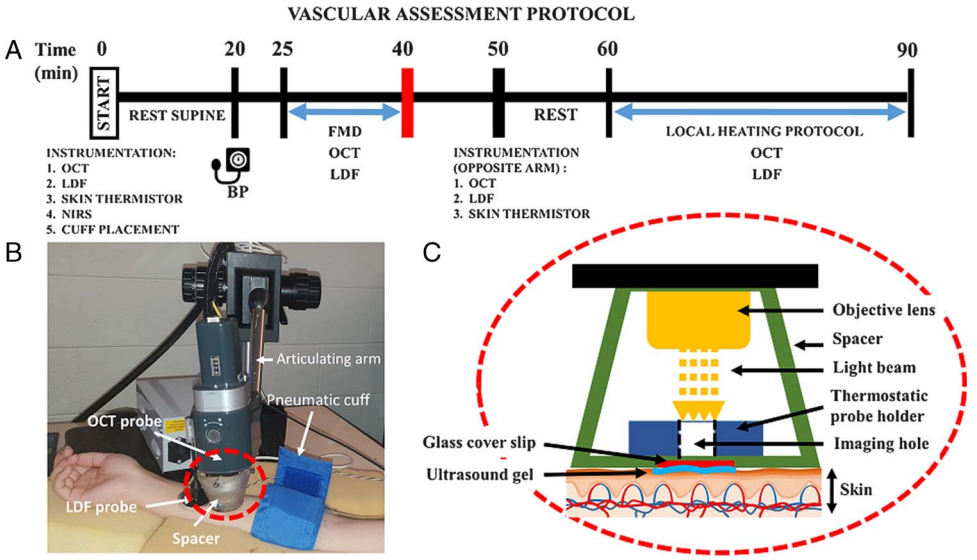

FIGURE 1—Illustration of the timeline of vascular assessment protocol (A), instrumentation for OCT and LDF probes and skin microvascular assessment in the FMD protocol (B), and schematic diagram of OCT probe (imaging head)–skin tissue interface (C).

with transparent plastic and the OCT/LDF sites were again drawn using Henna dye. Photographs were also taken, and distances from anatomical landmarks recorded. Repeated measures were therefore collected at the same site in each subject.

Skin microvascular assessment during reactive hyperemia was assessed simultaneously with brachial artery FMD assessment, as described previously. A resting OCT image was obtained over 5 × 5 × 2.5-mm field of view (FOV). The FOV here is defined as (x,y,z), where z is in the direction of the light beam and x,y are approximately parallel to the skin surface. Postocclusion OCT scans were performed 30 s after the cuff deflation to capture the reactive hyperemic responses using a smaller FOV (2.5 × 2.5 × 2.5 mm) to optimize the timing of assessment. LDF baseline and postocclusion assessments were captured and analyzed using the same time window (90 s at baseline and 30 s during reactive hyperemia), to ensure consistency with the OCT measures.

After a further 10-min rest, assessment of the skin microvasculature in response to a local heating protocol was completed on the opposite arm to that exposed to the reactive hyperemia stimulus. An LDF probe was again affixed to the central bore of thermostatic holder (PeriTemp 4005 Heater; Perimed, Stockholm, Sweden) with an adjacent OCT probe also affixed. OCT images were taken over a 5 × 5 × 2.5-mm FOV for local heating. Once the resting OCT scan was processed, a local rapid heating protocol (1°C per 10 s, from 33°C to 44°C, then 30 min at 44°C) commenced (30,39). Final OCT heating data were obtained at the end of 30 min of the local heating protocol. LDF-derived blood flux at either baseline or at the end of 30-min local heating was calculated across the same time point (90-s bin) as OCT scans for comparative purposes.

OCT image acquisition and analysis. The OCT-derived image acquisition and analysis are described in detail in our methodological articles (29,30), and a brief summary is provided here. OCT data were acquired at a sampling resolution of 5 × 1 × 2.5 μm (X × Y × Z), where the X and Y dimensions are approximately parallel to the skin surface and the Z dimension is orientated into the skin. The focus of the OCT light beam was set to a depth of approximately 300 μm below the skin surface to optimize the image quality over the first 600-μm depth. Individual OCT measurements (A-scan) were acquired at a rate of 76 kHz, and the total acquisition time was approximately 90 s for large FOV and 30 s for smaller FOV. We found this acquisition time to be well tolerated by our subjects, with minimal movement artifact. The stack of A-scans was collected and speckle decorrelation analysis performed to distinguish blood vessels from surrounding tissue using an automated analysis algorithm. The statistical characteristics of the speckle noise are related to blood flow speed, with faster blood flow giving rise to more rapid fluctuations in the speckle noise. By quantifying the characteristics of the speckle noise, we were able to compute an estimate of flow speed at each OCT voxel. Using standard imaging processing techniques, voxels containing flow were then aggregated into vessels, providing a two-dimensional projection image of the vasculature parallel to the skin surface. We calculated the average vessel diameter (units: micrometers) and average flow speed within vessels (units: micrometers per second) over the entire scanning FOV. We also computed the average flow in each vessel (units: picoliters per second). Finally, we computed an estimate of vessel density by generating a two-dimensional projection image of the blood vessels (as shown in Fig. 2) and quantifying the pixels that lay on a blood vessel as a percentage of the total FOV.

The OCT-derived diameter, speed, flow rate, and density are reported at baseline and in response to reactive hyperemia and local heating. All OCT and LDF-derived parameters are also presented as an increase (Δ) from the preceding baseline, with the exception of OCT-derived parameters in response to reactive hyperemia, because different FOV values were used to facilitate rapid assessment after cuff deflation.

Statistical Analysis

The calculation of sample size was based on the published data of Atkinson et al. (26), which reported skin microvascular responses before and after 8 wk of exercise training. Based on the effect size in that experiment and assuming $\alpha = 0.05$ and $\beta = 0.8$, the minimum number of subjects required to establish a significant change in the cutaneous vascular conductance response to skin heating stimulation was determined at seven per group (G*power, version 3.1.9.7).

Statistical analysis was performed using PRISM 8.1 (GraphPad, La Jolla, CA). The results are reported as means and SD, unless stated otherwise. Statistical analysis was performed using two-way ANOVA to calculate differences between groups, with a repeated measure pretraining versus posttraining. When ANOVA tests were significant, *post hoc* analysis using Fisher's least significant differences was used to assess changes. Further FMD analysis, which included SR_{AUC} as a time-varying covariate, was performed via linear-mixed modeling in STATA 15.0 (STATA Corporation LP, College Station, TX). Results are statistically significant if $P < 0.05$.

RESULTS

Participants characteristics. Participant characteristics before (week 0) and after (week 8) intervention are presented in Table 1. Age, resting blood pressure, resting heart rate (RHR), body weight, and BMI did not differ between groups at baseline (Table 1, week 0). There was no significant (time–group) interaction for systolic blood pressure (SBP), diastolic blood pressure (DBP), mean arterial pressure (MAP), or heart rate (two-way ANOVA: SBP, $P = 0.454$; DBP, $P = 0.791$; MAP, $P = 0.813$; RHR, $P = 0.395$), suggesting that there were no divergent responses in these outcomes in the two groups. However, there were significant main effects for resting SBP (time effect, $P = 0.01$; group effect, $P = 0.03$), suggesting that SBP decreased after intervention and that SBP in the training group was lower across both time points than in controls. *Post hoc* analysis subsequent to the main effect for time revealed that SBP was significantly lower relative to its baseline in the training group (post 108 ± 5 mm Hg vs pre

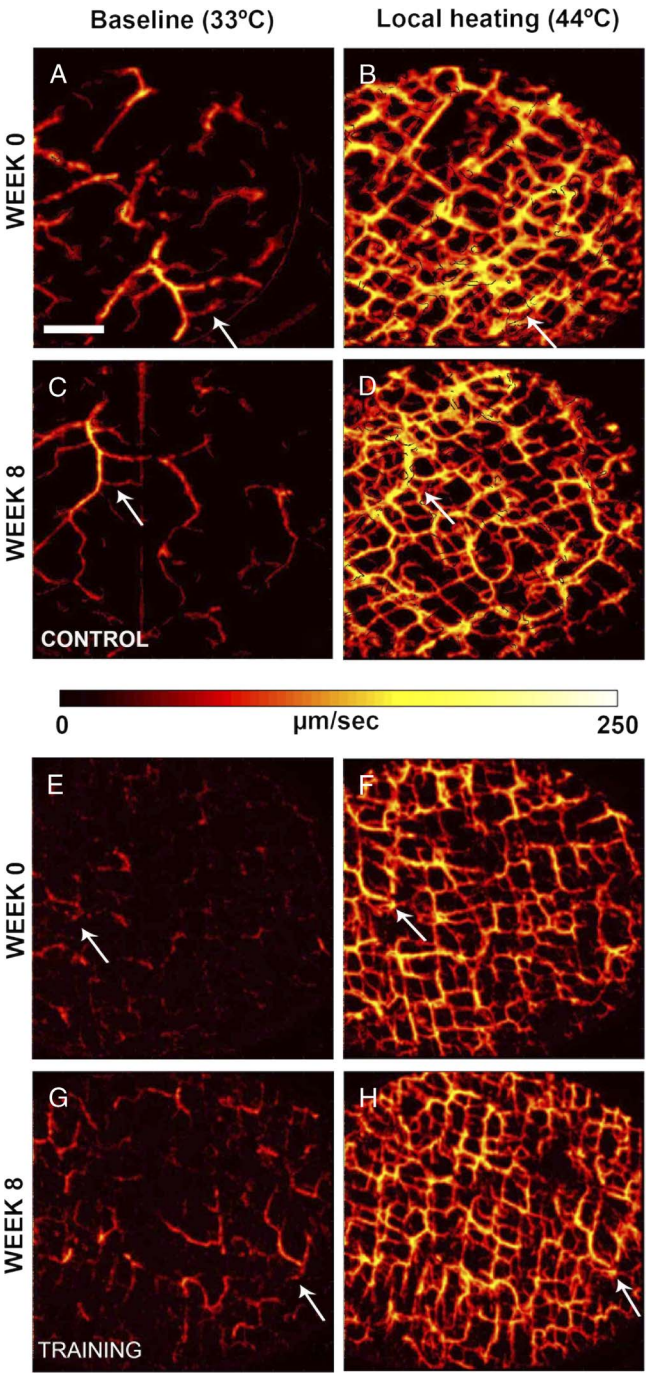

FIGURE 2—Representative OCT-derived images from forearm skin microvessels at baseline (left panel (A, C, E, G), 33°C) and at the point of maximal local heating (right panel (B, D, F, H), 44°C) in a control (top panel) and exercise-trained subject (bottom panel). *White arrows* point to similar sites assessed in these individuals at the study entry (week 0) and during the repeated OCT scan after exercise training or control interventions (week 8). Blood vessels are color coded to indicate flow speed (in micrometers per second). The *white scale* bar represents 500 µm.

113 ± 6 mm Hg, *post hoc* $P = 0.019$) but not the controls ($P = 0.144$). *Post hoc* analysis subsequent to the main effect for group revealed that SBP was significantly lower only for the posttraining time point (training: 108 ± 5 mm Hg vs control: 115 ± 6 mm Hg, $P = 0.019$) but not at baseline (training: 113 ± 6 mm Hg vs control: 118 ± 5 mm Hg, $P = 0.089$). In any event, all measures of SBP were within the normal range.

In keeping with these results for SBP, there was a significant time effect for resting MAP ($P = 0.012$), whereas group effect was borderline significant ($P = 0.053$), suggesting that MAP decreased after the intervention period across groups. *Post hoc* analysis subsequent to this main effect for time revealed a significant reduction in MAP relative to its baseline in the training group (post 77 ± 4 mm Hg vs pre 81 ± 5 mm Hg, *post hoc* $P = 0.044$) but not the controls ($P = 0.082$). There was also a significant main effect for time for resting DBP ($P = 0.048$) but no group effect ($P = 0.08$). *Post hoc* analysis subsequent to this effect showed no significant reduction in DBP relative to its baseline in either group (all, $P \geq 0.05$). Similarly, there was a significant time effect for RHR ($P = 0.014$) but no group effect ($P = 0.118$), suggesting that RHR decreased after intervention across groups. *Post hoc* analysis subsequent to this main effect revealed a significant reduction in RHR relative to its baseline in the training group (post 60 ± 3 bpm vs pre 66 ± 8 bpm, *post hoc* $P = 0.021$) but not in the controls ($P = 0.198$). No changes were evident in body weight or BMI after training (two-way ANOVA, interaction and main effect, $P \geq 0.05$).

Effect of exercise training on cardiorespiratory fitness ($\dot{V}O_{2max}$). The two-way ANOVA for $\dot{V}O_{2max}$ revealed a significant interaction effect ($P < 0.001$, Table 1) and time effect ($P = 0.001$) but no group effect ($P = 0.11$), whereby $\dot{V}O_{2max}$ increased after 8 wk of training (post 36.3 ± 2.6 $mL \cdot kg^{-1} \cdot min^{-1}$ vs pre 29.7 ± 2.8 $mL \cdot kg^{-1} \cdot min^{-1}$, *post hoc* $P < 0.001$), and the posttraining value was significantly higher compared with the control group (29.1 ± 5.4 $mL \cdot kg^{-1} \cdot min^{-1}$, *post hoc* $P = 0.002$). No change of $\dot{V}O_{2max}$ was evident in the control group ($P = 0.442$). There was no significant interaction or group effect for HR_{max}, but the time effect was significant ($P = 0.002$), whereby HR_{max} posttest was lower in both the training and control groups at week 8 (training group: post 178 ± 8 bpm vs pre 184 ± 12 bpm, *post hoc* $P = 0.023$; control group: post 179 ± 9 bpm vs pre 185 ± 11 bpm, *post hoc* $P = 0.023$). However, the maximal exercise time and power achieved at max improved only in the training group ($Time_{max}$ interaction effect, $P = 0.003$: post 16.9 ± 3.4 min vs pre 13.7 ± 2.3 min, *post hoc* $P = 0.001$; $Power_{max}$ interaction effect, $P = 0.005$: post 185 ± 33.4 W vs pre 165 ± 33.4 W, *post hoc* $P = 0.001$). Posttraining data were also higher compared with the control group ($Time_{max}$, 13.5 ± 1.6 min, *post hoc* $P = 0.007$; $Power_{max}$, 143 ± 14.1, *post hoc* $P = 0.004$). No changes were evident in either $Time_{max}$ or $Power_{max}$ in the control group (all, $P \geq 0.05$).

Effect of exercise training on body composition. In absolute terms, visceral adipose tissue, total and area-based fat and lean mass, and bone mineral density were not altered after 8 wk of training (Table 2). In relative terms (%), there was no significant interaction effect for the percentage of total or area-based fat and lean mass, or bone mineral density. However, there was a significant time effect for percentage gynoid

TABLE 2. Body composition.

	Control (n = 8, ♂)		Training (n = 8, ♂)		RM 2-Way ANOVA, P Value		
	Week 0	Week 8	Week 0	Week 8	Time	Group	Interaction
Fat							
Total, kg	26.1 ± 8.8	26.4 ± 8.5	23.0 ± 7.4	21.7 ± 7.2	0.306	0.347	0.113
Total, %	33.1 ± 6.5	33.1 ± 5.6	31.3 ± 6.3	25.8 ± 12.2	0.188	0.215	0.191
Android, kg	2.4 ± 1.1	2.4 ± 1.1	2.1 ± 0.8	1.9 ± 0.8	0.23	0.478	0.198
Android, %	40 ± 10.5	40.6 ± 8.7	38.3 ± 10.6	36.1 ± 10.3	0.283	0.542	0.082
Gynoid, kg	4.3 ± 1.4	4.3 ± 1.4	4.1 ± 2.2	3.4 ± 1.3	0.117	0.495	0.212
Gynoid, %	34.1 ± 6.2	33.6 ± 5.7	30.8 ± 6.8	28.8 ± 6.6*	0.013	0.221	0.111
Visceral adipose tissue, g	805.9 ± 526.4	819.5 ± 567.9	649.1 ± 299.7	599.5 ± 264.7	0.67	0.393	0.457
Lean mass, kg							
Total, kg	50.9 ± 6.6	51.0 ± 6.8	48.9 ± 6.5	49.4 ± 6.4	0.261	0.585	0.422
Total, %	66.9 ± 6.5	66.9 ± 5.6	68.7 ± 6.3	70.3 ± 6.1	0.087	0.407	0.092
Arms, kg	5.5 ± 0.9	5.5 ± 0.9	5.3 ± 0.7	5.3 ± 0.7	0.459	0.665	0.71
Arms, %	71.0 ± 5.6	70.7 ± 6.1	71.7 ± 5.4	72.8 ± 5.3	0.299	0.608	0.099
Leg, kg	19.4 ± 3.2	19.7 ± 3.3	18.2 ± 3.1	18.5 ± 3.1	0.022	0.471	0.704
Leg, %	69.7 ± 5.8	70.1 ± 5	72.1 ± 5.4	73.8 ± 5.5*	0.007	0.274	0.089
Trunk, kg	22.2 ± 2.4	21.9 ± 2.6	21.7 ± 2.4	21.9 ± 2.5	0.813	0.828	0.133
Trunk, %	62.4 ± 8.3	62.1 ± 6.8	64.4 ± 8.3	66.1 ± 8	0.117	0.291	0.117
Bone mineral density							
Total, g·cm^{-2}	1.27 ± 0.15	1.28 ± 0.16	1.22 ± 0.06	1.22 ± 0.05	0.554	0.369	0.09
Bone mineral content, g	2691.4 ± 456.3	2703.6 ± 464.4	2492.5 ± 379.3	2504.2 ± 388.3	0.148	0.363	0.975

Values are mean ± SD.
*P < 0.05, week 0 vs week 8 within the group.
RM, repeated-measures.

fat mass (P = 0.013) and leg lean mass (P = 0.007), independent of a group effect (percent gynoid fat mass, P = 0.221; percent leg lean mass, P = 0.274), suggesting that decreased % gynoid fat mass and increased percent leg lean mass after the intervention period were observed in both groups. *Post hoc* analysis subsequent to the main effect for time revealed a significant reduction in percent gynoid fat mass relative to its baseline in training group (post 28.8% ± 6.6% vs pre 30.8% ± 6.8%, *post hoc* P = 0.006) but not in the controls (P = 0.198). In keeping with this, percent leg lean mass increased relative to its baseline in the training group (post 73.8% ± 5.5% vs pre 72.1% ± 5.4%, *post hoc* P = 0.003) but not in the controls (P = 0.354). Percentages of total/android fat mass and total/arm/trunk mass were not altered, although the results revealed a consistent trend after training for reduced percent fat mass and an increase in lean mass (all, $P \geq 0.05$).

Effect of exercise training on vascular endothelial function. Baseline brachial artery diameter did not change in either the training or control group (two-way ANOVA interaction, P = 0.945; time, P = 0.422; group, P = 0.354). There was a significant interaction (P = 0.04) but no main effect, for FMD (time effect, P = 0.075; group effect, P = 0.21) whereby increase in FMD was observed after training (post 9.83% ± 3.27% vs pre 6.97% ± 1.77%, *post hoc* P = 0.01), with this posttraining value being higher compared with the control group (6.9% ± 2.87%, *post hoc* P = 0.027). No change in FMD was evident in the control group (P = 0.894). Mixed-model analyses showed significant time (P = 0.003) and interaction (P = 0.008) effects for FMD, after SR_{AUC} was accounted for as a time-varying covariate. Brachial blood flow, at baseline, peak, or the increase after a 5-min period of

TABLE 3. Impact of 8-wk cycling on brachial artery characteristics and skin microvascular reactivity (LDF-derived parameters).

	Control (n = 8, ♂)		Training (n = 8, ♂)		RM 2-Way ANOVA, P Value		
	Week 0	Week 8	Week 0	Week 8	Group	Time	Interaction
Brachial artery							
Diameter							
Baseline, mm	3.73 ± 0.22	3.81 ± 0.47	3.91 ± 0.42	3.97 ± 0.43	0.354	0.422	0.945
FMD, % baseline	7.14 ± 1.74	6.90 ± 2.87	6.97 ± 1.77	9.83 ± 3.27*,**	0.21	0.075	0.04
SR_{AUC} (in 10^3)	17.9 ± 9.7	21.8 ± 10.8	19.4 ± 12.9	20.5 ± 11.6	0.981	0.355	0.609
Flow							
Baseline, mL·min^{-1}	25.3 ± 10.7	36.0 ± 26.8	31.3 ± 15.3	35.7 ± 22.7	0.74	0.171	0.558
Peak, mL·min^{-1}	301.2 ± 115.9	334.5 ± 149.7	281.2 ± 93.2	328.8 ± 65.2	0.806	0.07	0.733
Δ Flow, mL·min^{-1}	275.9 ± 109.5	298.5 ± 132.6	249.8 ± 86.2	293.1 ± 59.2	0.102	0.741	0.592
Skin microvascular reactivity (LDF)							
Local heating							
Baseline, PU·mm Hg^{-1}	0.17 ± 0.08	0.15 ± 0.08	0.14 ± 0.06	0.16 ± 0.06	0.643	0.884	0.323
Peak LH, PU·mm Hg^{-1}	1.38 ± 0.27	1.33 ± 0.19	1.59 ± 0.57	1.54 ± 0.23	0.112	0.704	0.988
Δ BL-LH, PU·mm Hg^{-1}	1.21 ± 0.25	1.18 ± 0.15	1.45 ± 0.55	1.38 ± 0.23	0.089	0.694	0.872
Postocclusive reactive hyperemia							
Baseline, PU·mm Hg^{-1}	0.19 ± 0.10	0.18 ± 0.10	0.2 ± 0.09	0.24 ± 0.11	0.436	0.646	0.549
$RH_{30-60\ s}$ CVC, PU·mm Hg^{-1}	0.49 ± 0.30	0.54 ± 0.30	0.47 ± 0.16	0.70 ± 0.37	0.583	0.162	0.315
Δ BL-RH, PU·mm Hg^{-1}	0.31 ± 0.22	0.35 ± 0.24	0.27 ± 0.14	0.46 ± 0.26	0.69	0.088	0.274

Values are mean ± SD.
*P < 0.05, week 0 vs week 8 within the same group.
**P < 0.05, between groups at the same time point.
CVC, cutaneous vascular conductance; RH, reactive hyperemia; RM, repeated-measures.

local ischemia period, was unaltered after training (all, $P \geq 0.05$; Table 3).

Effect of exercise training on skin microvascular characteristics. Figure 2 is representative of OCT-derived images at rest (baseline) and in response to 30 min of local heating, collected at Henna-marked sites from one individual in the control and training groups. Baseline OCT-derived diameter, speed, flow rate, and density were not different after training (Fig. 3). There was a significant interaction for local heating-induced OCT-derived speed (P = 0.038), whereby a significant decrease at peak heating was observed after training (post 98.6 ± 3.9 $\mu m \cdot s^{-1}$ vs pre 102 ± 5 $\mu m \cdot s^{-1}$, *post hoc* P = 0.012; Fig. 3Bii), whereas no change in OCT-derived speed was observed in the control group (P = 0.877; Fig. 3Bi). However, no differences were apparent when changes with heating were compared between these groups (Fig. 3Biii). Other local heating-induced OCT parameters (diameter, flow rate, and density) were not altered after training (Fig. 3). In keeping with these OCT results, skin conductance derived from LDF measures also did not reveal any differences at baseline, at peak, or in the magnitude of local heating responses (Table 3). OCT (Fig. 4) and skin conductance (Table 3) parameters

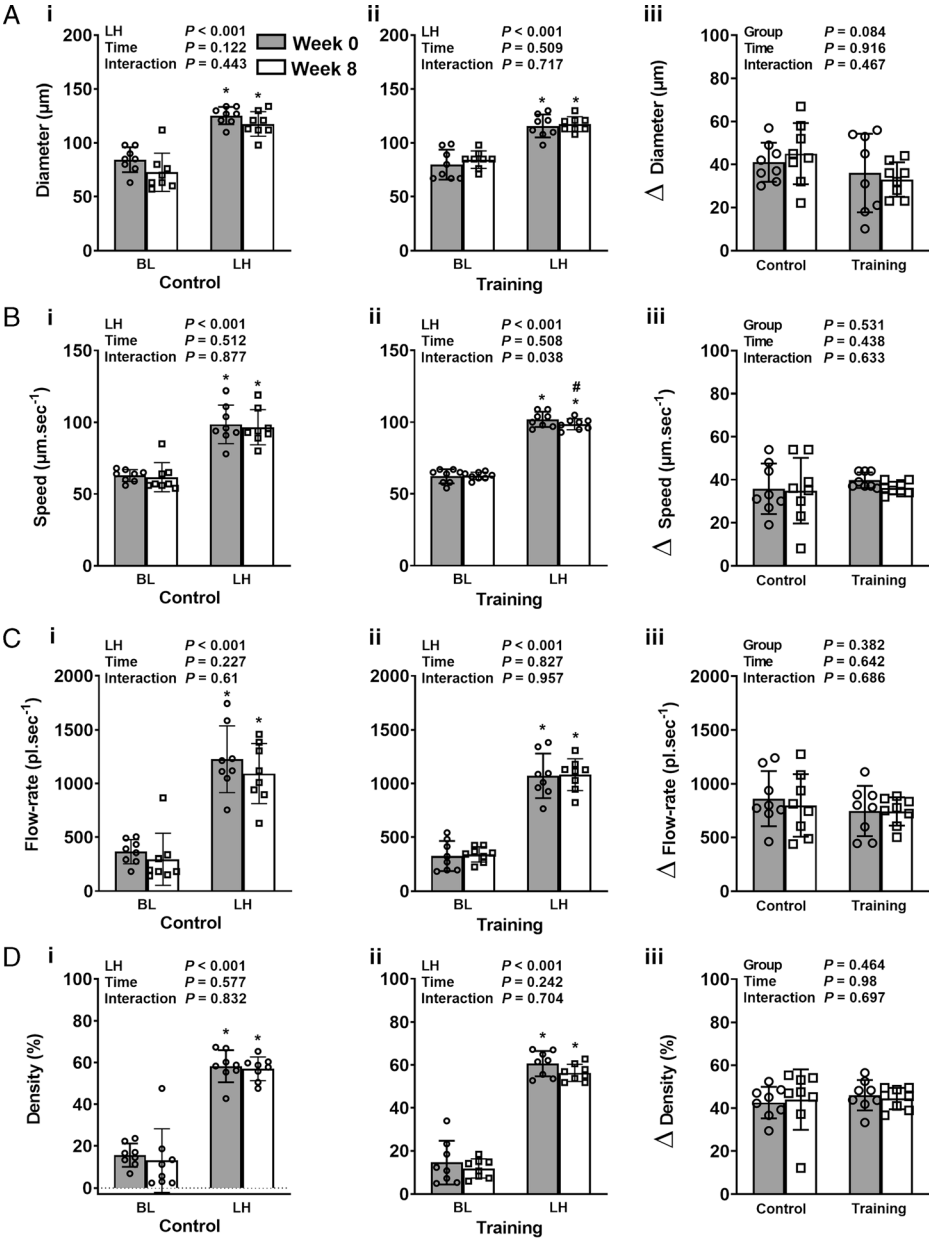

FIGURE 3—OCT-derived parameters (A: diameter, B: speed, C: flow rate, and D: density) before and after intervention, at baseline (BL) and the at the end of 30 min prolonged local heating (LH), in the control (i) and training (ii) groups. The magnitude of local heating responses are shown as the increment of each parameter relative to their baseline (Δ LH-BL, iii). Values are presented in means ± SD. A two-way repeated-measures ANOVA was performed to compare local heating responses within groups (i and ii panels: LH–time) and the magnitude of local heating responses between group (iii panels: group–time) for all OCT-derived parameters. *P < 0.05 LH responses vs BL within same time point. #P < 0.05 LH heating responses week 0 vs week 8 within the group.

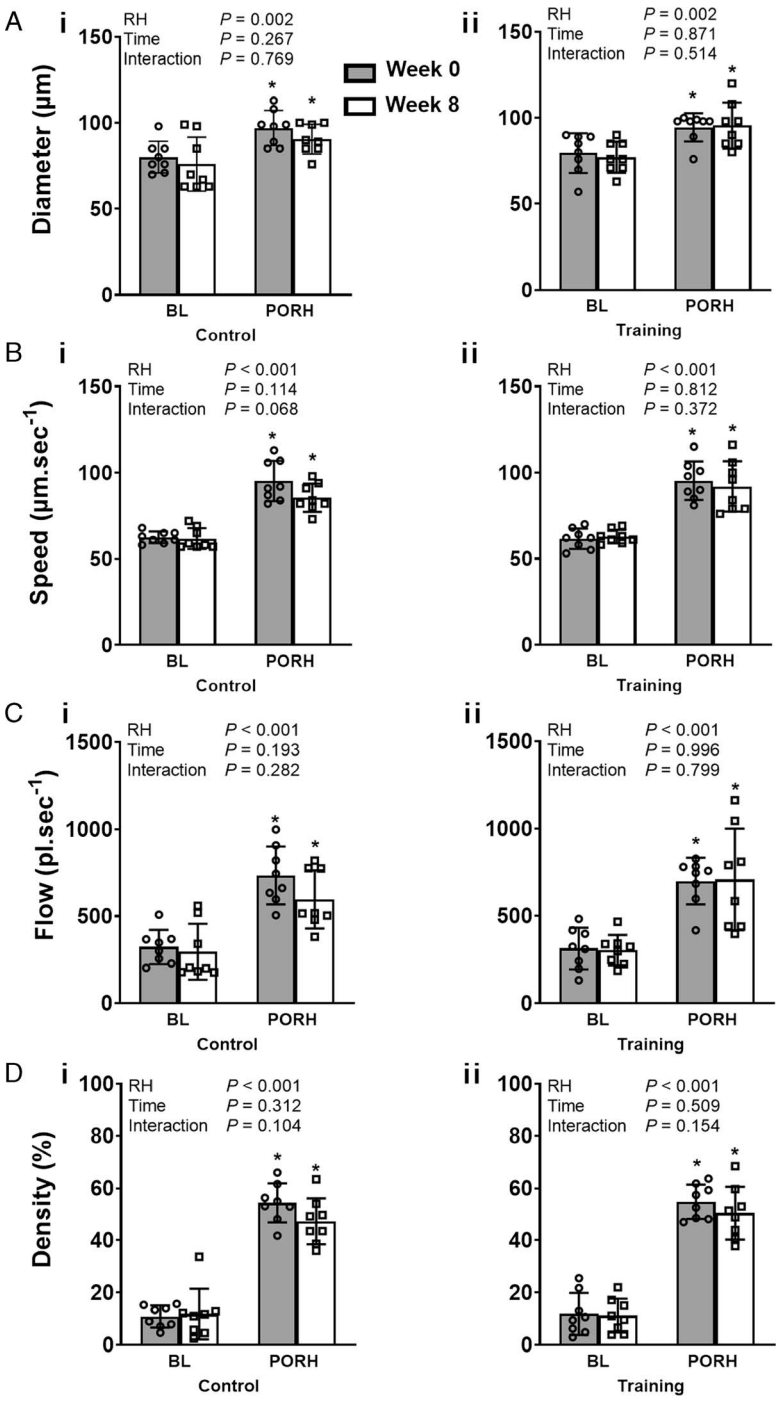

FIGURE 4—The effect of exercise training on OCT-derived parameters (A: diameter, B: speed, C: flow rate, and D: density) at baseline (BL) and in response to postocclusion reactive hyperemia (PORH), in the control (i) and training (ii) groups. Values are presented as mean ± SD. A two-way repeated-measures ANOVA was performed to compare reactive hyperemia (RH) responses before and after exercise training intervention (Interaction = RH–time) for all OCT-derived parameters. *$P < 0.05$ RH responses vs BL within same time point.

were unaltered after exercise training in response to reactive hyperemia.

DISCUSSION

Our study revealed that 8 wk of aerobic cycle ergometer training in young healthy subjects improved fitness, body composition, BP, HR, and conduit (brachial) artery function compared with inactive controls. In contrast, training did not markedly affect OCT-derived responses of the cutaneous microcirculation. Although our FMD data are broadly consistent with previous studies on the effect of training in larger arteries (10), our use of a new OCT-based imaging technique to visualize and quantify skin microvessels revealed findings that lead us to reject our hypothesis that repeated increases in blood flow induce microvascular adaptation in the skin.

In response to exercise training, conduit and larger skeletal muscle resistance arteries that control blood flow exhibit functional and structural adaptation that is largely mediated by repeated episodic increases in shear stress (3,4,12). It is also well established that skeletal muscle capillary beds exhibit angiogenic adaptation to exercise training (16). Our finding in healthy subjects suggests that the skin does not adapt in a similar manner, despite the fact that, like active skeletal muscle, cutaneous blood flow increases significantly in response to exercise (40). Our findings suggest that blood flow and shear stress may not be key mediators of structural microvascular adaptation in skin microvessels, and that other stimuli such as hypoxia may be more important. Indeed, transient hypoxia in skeletal muscle induces the release of the proangiogenic substances during exercise (16,41,42), whereas the skin remains hyperperfused relative to metabolism as a consequence of thermoregulation (43). Although no study to date has examined the effect of exercise on the release of cutaneous angiogenic proteins, it is known that individuals with severely impaired cutaneous perfusion (and therefore hypoxia), such as diabetic patients (39,44), display profound structural differences in their cutaneous microvessels. Future studies of exercise training in clinical populations are warranted.

An important consideration when discussing the findings of previous studies is the differing terminology used for the segments of the vascular tree. For example, previous studies (10,45) have demonstrated that exercise training improves endothelial function in both conduit and "resistance" arteries. The latter studies have relied on blood flow measures derived from limb plethysmography or conduit artery quantitative duplex ultrasound, whereby changes in flow are a surrogate for "resistance vessel" function (46). The arteries that control limb flow and resistance are likely to be larger than the precapillary vessels we imaged in the skin (47), raising the possibility that larger resistance arterioles behave and respond differently to smaller microvessels. This is consistent with reports that larger vessels adapt structurally via caliber enlargement, whereas small microvessels undergo angiogenesis via budding and sprouting of new vessels (48). From a physiological perspective, it is reasonable to conceptualize the arterial tree as consisting of larger elastic arteries, conduit arteries, resistance arterioles, and microvessels. Although such classification may not be consistent with the commonplace depiction of "resistance vessels" as encompassing all those between conduit arteries and capillaries, it is nonetheless consistent with known differences that exist in artery wall anatomy (49).

Despite the limitations of laser Doppler technology, which does not image actual microvessels, some previous studies have attempted to assess microvascular adaptation to exercise in the skin, with mixed results. Individuals with higher fitness levels demonstrate enhanced endothelium-dependent vasodilation compared with less fit controls in some (19) but not all (20) studies. The sole-author article of Wang (22) reported increased skin blood flow at rest, as a response to incremental exercise, and endothelium-dependent vasodilation after 8 wk of exercise training in young healthy, sedentary people, and this effect was reversed to pretraining state after detraining. Enhanced NO contribution to skin vasodilation after training has been reported in young type 2 diabetic subjects (5), and Black et al. (23) demonstrated, using LDF combined with microdialysis of NO blockade, that the NO contribution to skin flux responses increased after exercise training in the sedentary elderly subjects, suggesting that exercise training can enhance microvasculature function. However, Atkinson et al. (26) reported decreased LDF-based responses to local heating after exercise training, an adaptation that was associated with repeated increases in shear stress, as changes were not apparent in the contralateral forearm in which shear stress was clamped during exercise. We therefore speculated in Atkinson et al. that the training-induced decrease in skin red cell flux by LDF may have been caused by angiogenic adaptation. Although we are not able to reproduce the decrease in LDF-derived variables (cutaneous vascular conductance) in our study, somewhat in keeping with the findings of Atkinson et al., we observed a decrease in the response to local heating of OCT-derived speed after training in the present study, and this response was not apparent in the control group. There are some important differences between the current study and Atkinson et al. that may contribute to the different results. In the latter, we utilized a longer local heating protocol (±2.5 h) by slowly increasing disk heat to 42°C and 44°C, whereas we simplified the protocol in our current experiment by rapidly increasing the heating disk temperature to 44°C; our focus here was to reveal structural adaptation in skin microcirculation. These different local heating approaches may provoke distinct physiological responses (27,37,43,50,51). In addition, instead of the within-subject between-limb model exploited by Atkinson et al., we did a comparison of skin microcirculation between subject groups; therefore, we did not eliminate central factors such as circulating hormones, neural outflow, or sympathetic activity that might affect microcirculatory adaptation to training.

Although the precise effect of exercise training and change in blood flow on cutaneous vascular function remains to be elucidated, in the current experiment, we observed no unequivocal evidence to support our previous speculation in Atkinson et al. that exercise training may induce structural remodeling of the cutaneous vasculature. This observation suggests that changes in thermoregulatory function with exercise in humans may be unrelated to intrinsic structural changes in peripheral skin microvesssels. It is well established that exercise training induces a lower skin vasodilatory threshold (52,53). This was not influenced by changes in cutaneous sympathetic vasoconstriction, suggesting that active vasodilator mechanisms or changes in blood volume may be the main contributor to training-induced adaptation in skin blood flow control (53). Moreover, the magnitude of maximal vasodilation reached during exercise is increased after training (54,55), whereas previous studies have commonly shown that the slope (sensitivity) of the relation between core temperature–skin blood flow is not changed (52–54). Finally, the sympathetic neural control of the circulation may be altered by exercise training (52,56). Taken together with our findings, this suggests that local cutaneous vascular adaptations are not largely responsible

for training-induced changes in the control of skin blood flow and reinforces the concept that central adaptations to training, particularly changes in blood/plasma volume, may be the major contributor to training-induced thermoregulatory adaptation in humans (57,58).

This study had several limitations. Our sample size was relatively small; however, power was adequate as based on previous studies (26). In terms of OCT imaging, the assessment of skin microvessels was obtained from a small area and may not be a representative of other areas of the skin. Because skin microvascular density is heterogenous, different vascular beds may exhibit distinct responses (59). We also rendered the images in two dimensions, and the current OCT approach we use has relatively limited temporal resolution. It is likely that future development of OCT technology will overcome these issues and generate four-dimensional images in real time. It is also possible that exercise-induced adaptation in human microvessels depends on the time course of training, as is apparent in the conduit arteries (2–4). These exercise training studies revealed a biphasic pattern of functional change in conduit arteries, whereby the FMD increased after several weeks of training, then returned toward baseline as the increase of dilator capacity occurred. These findings suggest the occurrence of structural remodeling (2–4) and fit with Laughlin's (60) original proposal that initial improvement in vasodilator capacity contributes to normalizing the increase in shear stress during exercise, whereas continuing exercise leads to structural adaptation for more "permanent" shear stress normalization. Unfortunately, we did not assess brachial artery dilator capacity as a surrogate measure for conduit artery structure in the current study. Although functional and structural adaptation to exercise training in conduit arteries seems to be time dependent, the precise timeline of this adaptation is still not clearly defined and probably depends on dose and mode of exercise. With regard to the timing of adaptation in microvessels, White et al. (61) reported in the coronary microvasculature that initial increases in capillary growth and small arterioles density (<30 μm) reached a peak 3 wk after training onset and declined with longer training. We may therefore have missed microvascular adaptation in the skin at our 8-wk follow-up, despite observing improvement in brachial artery FMD. A further limitation is that, because of our focus on examining changes in cutaneous vascular structure (remodeling), we utilized a different local heating protocol from that used by some previous functionally orientated studies, and it is well established that different local heating approaches provoke distinct physiological responses (50,51). In addition, the effects of training on microvascular adaptation may depend on the subjects studied: those with impaired skin microvascular function (5,23,62), such as those with diabetes and those with cardiovascular diseases, may prove more responsive than the healthy young subjects we studied. Indeed, the effect of training on conduit and larger resistance vessels is more apparent in those with impaired arterial function *a priori* (63). Finally, our study involved local skin heating and intrinsic adaptations in the cutaneous vasculature; the effect of whole body heating on OCT-derived outcomes has not been studied and may differ, as systemic and neural regulatory changes have important impacts on thermoregulatory adaptation. Further studies (perhaps using OCT insights) will be required to address such integrative thermoregulatory questions.

CONCLUSIONS

Our findings suggest that vascular adaptation to exercise training in healthy young adults is not uniform across different levels of the arterial tree. Although exercise training improved larger artery function, this was not accompanied by unequivocal evidence for cutaneous microvascular adaptation. Our OCT approach provides insights not previously possible in humans and should be applied in future studies of different populations with *a priori* impairment in skin microvascular function.

We extend our gratitude to the participants and to Ms. Chariez Peter and Ms. Zhaoran Guo for their assistance with this study.

R. A. is supported by a scholarship from Indonesian Endowment Fund for Education, Ministry of Finance, Indonesia. R. A. M. is supported by a Premier's Research and Industry Fund grant provided by the South Australian Government Department for Industry and Skills. D. J. G. is supported by a National Health and Medical Research Council Principal Research Fellowship (APP1080914). This research is supported by grants from Australian Research Council (DP 130103793, DP 160104175, CE140100003). The Australian Research Council did not have any involvement in this study design, data collection or analysis of the results, or writing the report.

R. A. M. is a co-founder and Director of Miniprobes Pty Ltd, a company that develops novel optical imaging systems. Miniprobes Pty Ltd did not contribute to this study. The authors declare no conflicting interests, financial or otherwise. The results of present study do not constitute endorsement by American College of Sport Medicine. The results of the study are presented clearly, honestly, and without fabrication, falsification, or inappropriate data manipulation.

REFERENCES

1. Clarkson P, Montgomery HE, Mullen MJ, et al. Exercise training enhances endothelial function in young men. *J Am Coll Cardiol*. 1999; 33(5):1379–85.
2. Tinken TM, Thijssen DHJ, Black MA, Cable NT, Green DJ. Time course of change in vasodilator function and capacity in response to exercise training in humans. *J Physiol*. 2008;586(20):5003–12.
3. Tinken TM, Thijssen DHJ, Hopkins N, Dawson EA, Cable NT, Green DJ. Shear stress mediates endothelial adaptations to exercise training in humans. *Hypertension*. 2010;55(2):312–8.
4. Birk GK, Dawson EA, Atkinson C, et al. Brachial artery adaptation to lower limb exercise training: role of shear stress. *J Appl Physiol (1985)*. 2012;112:1653–8.
5. Naylor LH, Davis EA, Kalic RJ, et al. Exercise training improves vascular function in adolescents with type 2 diabetes. *Physiol Rep*. 2016;4(4):e12713.
6. Maiorana A, O'Driscoll G, Dembo L, et al. Effect of aerobic and resistance exercise training on vascular function in heart failure. *Am J Physiol Heart Circ Physiol*. 2000;279(4):H1999–2005.

7. Green DJ, Walsh JH, Maiorana A, et al. Comparison of resistance and conduit vessel nitric oxide–mediated vascular function in vivo: effects of exercise training. *J Appl Physiol (1985)*. 2004;97(2):749–55; discussion 748.
8. Rowley NJ, Dawson EA, Hopman MTE, et al. Conduit diameter and wall remodeling in elite athletes and spinal cord injury. *Med Sci Sports Exerc*. 2012;44(5):844–9.
9. Green DJ, Cable NT, Fox C, Rankin JM, Taylor RR. Modification of forearm resistance vessels by exercise training in young men. *J Appl Physiol (1985)*. 1994;77(4):1829–33.
10. Green DJ, Maiorana AJ, O'Driscoll G, Taylor J. Effects of exercise training on endothelium-derived nitric oxide function in humans. *J Physiol*. 2004;561(1):1–25.
11. Green D, Cheetham C, Mavaddat L, et al. Effect of lower limb exercise on forearm vascular function: contribution of nitric oxide. *Am J Physiol Heart Circ Physiol*. 2002;283(3):H899–907.
12. Green DJ, Hopman MTE, Padilla J, Laughlin MH, Thijssen DHJ. Vascular adaptation to exercise in humans: role of hemodynamic stimuli. *Physiol Rev*. 2017;97(2):495–528.
13. Atkinson CL, Carter HH, Naylor LH, et al. Opposing effects of shear-mediated dilation and myogenic constriction on artery diameter in response to handgrip exercise in humans. *J Appl Physiol (1985)*. 2015;119(8):858–64.
14. Hoier B, Nordsborg N, Andersen S, et al. Pro- and anti-angiogenic factors in human skeletal muscle in response to acute exercise and training. *J Physiol*. 2012;590(3):595–606.
15. Gliemann L, Buess R, Nyberg M, et al. Capillary growth, ultrastructure remodelling and exercise training in skeletal muscle of essential hypertensive patients. *Acta Physiol (Oxf)*. 2015;214(2):210–20.
16. Hoier B, Hellsten Y. Exercise-induced capillary growth in human skeletal muscle and the dynamics of VEGF. *Microcirculation*. 2014;21(4):301–14.
17. Rowell LB. Human cardiovascular adjustments to exercise and thermal stress. *Physiol Rev*. 1974;54(1):75–159.
18. Kvernmo HD, Stefanovska A, Kirkebøen KA, Østerud B, Kvernebo K. Enhanced endothelium-dependent vasodilatation in human skin vasculature induced by physical conditioning. *Eur J Appl Physiol Occup Physiol*. 1998;79(1):30–6.
19. Lenasi H, Strucl M. Effect of regular physical training on cutaneous microvascular reactivity. *Med Sci Sports Exerc*. 2004;36(4):606–12.
20. Veves A, Saouaf R, Donaghue VM, et al. Aerobic exercise capacity remains normal despite impaired endothelial function in the micro- and macrocirculation of physically active IDDM patients. *Diabetes*. 1997;46(11):1846–52.
21. Boegli Y, Gremion G, Golay S, et al. Endurance training enhances vasodilation induced by nitric oxide in human skin. *J Invest Dermatol*. 2003;121(5):1197–204.
22. Wang J-S. Effects of exercise training and detraining on cutaneous microvascular function in man: the regulatory role of endothelium-dependent dilation in skin vasculature. *Eur J Appl Physiol*. 2005; 93(4):429–34.
23. Black MA, Green DJ, Cable NT. Exercise prevents age-related decline in nitric-oxide-mediated vasodilator function in cutaneous microvessels. *J Physiol*. 2008;586(14):3511–24.
24. Pugh CJA, Cuthbertson DJ, Sprung VS, et al. Exercise training improves cutaneous microvascular function in nonalcoholic fatty liver disease. *Am J Physiol Endocrinol Metab*. 2013;305(1):E50–8.
25. Middlebrooke AR, Elston LM, MacLeod KM, et al. Six months of aerobic exercise does not improve microvascular function in type 2 diabetes mellitus. *Diabetologia*. 2006;49(10):2263–71.
26. Atkinson CL, Carter HH, Thijssen DHJ, et al. Localised cutaneous microvascular adaptation to exercise training in humans. *Eur J Appl Physiol*. 2018;118(4):837–45.
27. Carter HH, Spence AL, Atkinson CL, et al. Distinct impacts of blood flow and temperature on cutaneous microvascular adaptation. *Med Sci Sports Exerc*. 2014;46(11):2113–21.
28. Holowatz LA, Thompson-torgerson CS, Kenney WL. The human cutaneous circulation as a model of generalized microvascular function. *J Appl Physiol*. 2008;105(1):370–2.
29. Argarini R, Smith KJ, Carter HH, Naylor LH, McLaughlin RA, Green DJ. Visualizing and quantifying the impact of reactive hyperemia on cutaneous microvessels in humans. *J Appl Physiol (1985)*. 2020;128(1):17–24.
30. Smith KJ, Argarini R, Carter HH, et al. Novel noninvasive assessment of microvascular structure and function in humans. *Med Sci Sports Exerc*. 2019;51(7):1558–65.
31. Garber CE, Blissmer B, Deschenes MR, et al. Quantity and quality of exercise for developing and maintaining cardiorespiratory, musculoskeletal, and neuromotor fitness in apparently healthy adults: guidance for prescribing exercise. *Med Sci Sports Exerc*. 2011;43(7):1334–59.
32. Thijssen DHJ, Bruno RM, van Mil ACCM, et al. Expert consensus and evidence-based recommendations for the assessment of flow-mediated dilation in humans. *Eur Heart J*. 2019;40(30):2534–47.
33. Thijssen DHJ, Black MA, Pyke KE, et al. Assessment of flow-mediated dilation in humans: a methodological and physiological guideline. *Am J Physiol Heart Circ Physiol*. 2011;300(1):H2–12.
34. Woodman RJ, Playford DA, Watts GF, et al. Improved analysis of brachial artery ultrasound using a novel edge-detection software system. *J Appl Physiol (1985)*. 2001;91(2):929–37.
35. Lorenzo S, Minson CT. Human cutaneous reactive hyperaemia: role of BKCa channels and sensory nerves. *J Physiol*. 2007;585(1):295–303.
36. Wong BJ, Wilkins BW, Holowatz LA, Minson CT. Nitric oxide synthase inhibition does not alter the reactive hyperemic response in the cutaneous circulation. *J Appl Physiol (1985)*. 2003;95:504–10.
37. Minson CT, Berry LT, Joyner MJ, Christopher T, Berry LT. Nitric oxide and neurally mediated regulation of skin blood flow during local heating. *J Appl Physiol (1985)*. 2001;97403:1619–26.
38. Liew YM, McLaughlin RA, Gong P, Wood FM, Sampson DD. In vivo assessment of human burn scars through automated quantification of vascularity using optical coherence tomography. *J Biomed Opt*. 2013;18(6):061213.
39. Argarini R, McLaughlin RA, Joseph SZ, et al. Optical coherence tomography: a novel imaging approach to visualize and quantify cutaneous microvascular structure and function in patients with diabetes. *BMJ Open Diabetes Res Care*. 2020;8(1):e001479.
40. Joyner MJ, Casey DP. Regulation of increased blood flow (hyperemia) to muscles during exercise: a hierarchy of competing physiological needs. *Physiol Rev*. 2015;95(2):549–601.
41. Gustafsson T, Puntschart A, Kaijser L, Jansson E, Sundberg CJ. Exercise-induced expression of angiogenesis-related transcription and growth factors in human skeletal muscle. *Am J Physiol Heart Circ Physiol*. 1999;276(2):H679–85.
42. Tang K, Breen EC, Wagner H, Brutsaert TD, Gassmann M, Wagner PD. HIF and VEGF relationships in response to hypoxia and sciatic nerve stimulation in rat gastrocnemius. *Respir Physiol Neurobiol*. 2004;144(1):71–80.
43. Johnson JM, Minson CT, Kellogg DL. Cutaneous vasodilator and vasoconstrictor mechanisms in temperature regulation. *Compr Physiol*. 2014;4(1):33–89.
44. Adamska A, Pilacinski S, Zozulinska-Ziolkiewicz D, et al. An increased skin microvessel density is associated with neurovascular complications in type 1 diabetes mellitus. *Diab Vasc Dis Res*. 2019; 16(6):513–22.
45. Thijssen D, De Groot P, Smits P, Hopman M. Vascular adaptations to 8-week cycling training in older men. *Acta Physiol (Oxf)*. 2007; 190(3):221–8.
46. Joyner MJ, Dietz NM, Shepherd JT. From Belfast to Mayo and beyond: the use and future of plethysmography to study blood flow in human limbs. *J Appl Physiol (1985)*. 2001;91(6):2431–41.
47. Segal SS. Cell-to-cell communication coordinates blood flow control. *Hypertension*. 1994;23:1113–20.
48. Brown MD. Exercise and coronary vascular remodelling in the healthy heart. *Exp Physiol*. 2003;88(5):645–58.
49. Rhodin J. Architecture of the vessel wall. In: Berne RM, Shepherd JT, Renkin EM, et al, editors. *Handbook of Physiology: The Cardiovascular System*. Bethesda, MD: American Physiological Society; 1980. pp. 1–31.

50. Choi PJ, Brunt VE, Fujii N, Minson CT. New approach to measure cutaneous microvascular function: an improved test of NO-mediated vasodilation by thermal hyperemia. *J Appl Physiol (1985)*. 2014;117:277–83.
51. Carter SJ, Hodges GJ. Sensory and sympathetic nerve contributions to the cutaneous vasodilator response from a noxious heat stimulus. *Exp Physiol*. 2011;96(11):1208–17.
52. Roberts MF, Wenger CB, Stolwijk JA, Nadel ER. Skin blood flow and sweating changes following exercise training and heat acclimation. *J Appl Physiol (1985)*. 1977;43(1):133–7.
53. Thomas CM, Pierzga JM, Kenney WL. Aerobic training and cutaneous vasodilation in young and older men. *J Appl Physiol (1985)*. 1999, 86(5):1676–86.
54. Takeno Y, Kamijo Y-I, Nose H. Thermoregulatory and aerobic changes after endurance training in a hypobaric hypoxic and warm environment. *J Appl Physiol (1985)*. 2001;91(4):1520–8.
55. Fritzsche RG, Coyle EF. Cutaneous blood flow during exercise is higher in endurance-trained humans. *J Appl Physiol (1985)*. 2000; 88(2):738–44.
56. Johnson JM. Physical training and the control of skin blood flow. *Med Sci Sports Exerc*. 1998;30(3):382–6.
57. Sawka MN, Convertino VA, Eichner ER, Schnieder SM, Young AJ. Blood volume: importance and adaptations to exercise training, environmental stresses, and trauma/sickness. *Med Sci Sports Exerc*. 2000; 32(2):332–48.
58. Simmons GH, Wong BJ, Holowatz LA, Kenney WL. Changes in the control of skin blood flow with exercise training: where do cutaneous vascular adaptations fit in? *Exp Physiol*. 2011;96(9):822–8.
59. Roustit M, Cracowski JL. Non-invasive assessment of skin microvascular function in humans: an insight into methods. *Microcirculation*. 2012;19(1):47–64.
60. Laughlin M. Endothelium-mediated control of coronary vascular tone after chronic exercise training. *Med Sci Sports Exerc*. 1995;27(8):1135–44.
61. White FC, Bloor CM, McKirnan MD, Carroll SM. Exercise training in swine promotes growth of arteriolar bed and capillary angiogenesis in heart. *J Appl Physiol (1985)*. 1998;85(3):1160–8.
62. Lanting SM, Johnson NA, Baker MK, Caterson ID, Chuter VH. The effect of exercise training on cutaneous microvascular reactivity: a systematic review and meta-analysis. *J Sci Med Sport*. 2017;20(2):170–7.
63. Maiorana A, O'Driscoll G, Taylor R, Green D. Exercise and the nitric oxide vasodilator system. *Sports Med*. 2003;33(14):1013–35.